POLITECNICO DI TORINO
Repository ISTITUZIONALE

Microwave Antenna Array Calibration via Simulated and Measured S-parameters Matching

(Article begins on next page)

28 May 2023

Microwave Antenna Array Calibration via Simulated and Measured S-parameters Matching

C. Origlia, D. O. Rodriguez-Duarte, J. A. Tobon Vasquez, F. Vipiana

Dept. Electronics and Telecommunications, Politecnico di Torino, Torino, Italy,

{cristina.origlia, david.rodriguez, jorge.tobon, francesca.vipiana}@polito.it

Abstract—This paper extends the validation of an innovative calibration framework for microwave imaging systems combining measured scattering parameters with numerically simulated ones. The aim is to improve the imaging operator accuracy by overcoming possible variations between the measurement system and its numerical model. Here, we investigate the possibility of reconstructing the transmission coefficients, measured at the antenna ports, employing a custom set of simulations where manufacturing tolerances are introduced. The experimental validation considers a microwave antenna array designed for brain imaging; each antenna is immersed in a brick of custom coupling medium whose dielectric properties variability is mainly analyzed. Further, the simulated dataset is provided by a high-fidelity full-wave electromagnetic tool, based on the finite element method, and coupled with a 3-D CAD model. This work presents an essential step forward in the whole calibration scheme, to then be able to estimate the electric field within the domain of interest, thus improve the imaging operator.

Index Terms—microwave imaging, measurements calibration, microwave antenna array, numerical modeling.

I. INTRODUCTION

Microwave imaging (MWI) techniques deal with the reconstruction of a dielectric contrast map of the imaged object, starting from electromagnetic (EM) field measurements collected at discrete points around the object under test through an array of antennas.

Among the main challenges achieving an MWI system, the imaging algorithm faces a non-linear and ill-posed inverse scattering problem [1]. Several solutions are proposed in the literature, differing in computational cost, type of application, and robustness; typically, iterative strategies update the numerical forward model solution towards the measured data until convergence; other faster reconstruction algorithms exploit linearized models, relying on the linear Born approximation (in case of weak scatterers) [2]–[5]. Whatever the strategy, the algorithm requires in input the incident electric field inside the domain of imaging (DOI), not directly measurable, while usually provided by an accurate simulation model.

Although modern EM simulators ensure high numerical accuracy, the imaging outcome is still affected by modeling errors due to slight variation in the real measurement system (e.g., manufacturing tolerances, positioning errors, usage environment changes, etc.), which must be compensated with some calibration method. For example, the most common calibration procedures act improving the match between the signals measured in a reference experimental test and the correspondent simulated data [3], [6], [7]. In [8] two measured cases (with and without a scatterer inside the DOI) are exploited to extract the resolvent kernel.

In this paper, an innovative calibration scheme is proposed performing the projection of the measured data, collected in a reference scenario, on a synthetic dataset; the latter is obtained through a parametric numerical model of the MWI system under test, accounting for expected physical alterations of it. This hybrid simulation-measurement (HS-M) method is intended to give an EM description of the system as close as possible to the real one, to finally enhance the incident field estimation. The scheme takes inspiration from [9], where a similar mathematical background is applied in a reduced approach for antenna testing.

The validation here refers to the MWI device for brain stroke diagnosis and monitoring presented in [10] and experimentally validated in [11], which employs an in-house full-wave software based on the finite element method (FEM) as a high-fidelity numerical tool [12]. However, the proposed methodology is adaptable to different device layouts and MWI algorithms. Furthermore, its offline implementation is ideal while performing real-time imaging, as in the case of the above medical device. A preliminary study is given in [13], where the reconstruction of the antenna reflection coefficient was investigated. Instead, in this contribution, the investigation is applied to measured transmission coefficients (TCs) between different radiating elements, essential step to then estimate the electric field within the domain of interest in order to improve the used imaging operator.

II. HS-M CALIBRATION THEORY

The intended calibration scheme aims to dynamically match the numerical model, built from a priori information on the system, and the measured data, i.e. the S-parameters at the antenna ports. In practice, the method intends to describe the real behaviour of the system as a point in the space of all the possible solutions considering the expected variations in the experimental setup.

The following gives the main steps of the process, referring to the formulation previously detailed in [13].

First, a basis of synthetic data is provided in order to describe the scenario under test accounting for the expected variations from the nominal setting. Considering one transmitting (Tx) antenna, we collect the TCs with all the receivers in the array, simulated in several slightly altered scenarios

$$[S^{\text{sim}}] = [[S^{\text{sim}}_1], \cdots, [S^{\text{sim}}_K]], \qquad (1)$$

where K is the number of simulations and the k-th column vector $[S^{\text{sim}}_k]$ contains (NN_f) TCs, having N receivers and N_f frequency points. Thus, the basis functions are derived from the singular value decomposition (SVD) of $[S^{\text{sim}}]$, as the $(NN_f) \times K$ orthogonal matrix of left singular vectors

$$[\Psi] = [[\Psi_1], \cdots, [\Psi_K]]. \qquad (2)$$

Hence, the S-parameters measured in the real system for the Tx antenna, $[\tilde{S}]$, can be approximated (except for reconstruction errors) as a finite linear combination of the basis functions with unknown coefficients α:

$$[\tilde{S}] \cong [\Psi][\alpha], \qquad (3)$$

where $[\tilde{S}]$ is a (NN_f) vector and $[\alpha]$ collects K calibration coefficients. The "matching" process estimates the unknown coefficients by projecting the measured data on the given synthetic basis as follows:

$$[\alpha] = [\Psi]^\dagger[\tilde{S}], \qquad (4)$$

where † referred to the Moore-Penrose pseudo inverse, exploited to get the least-squares solution. In other words, the calibration coefficients allow the reconstruction of the antenna parameters $[S]$ starting from the simulated ones

$$[S] = [S^{\text{sim}}][\beta][\alpha], \qquad (5)$$

where β, is a $K \times K$ matrix introduced in [13] such that

$$[\Psi] = [S^{\text{sim}}][\beta]. \qquad (6)$$

Finally, assuming the linear relation between the sampled fields available at the antenna ports and the field radiated by the Tx antenna, the above coefficients can be equivalently applied obtaining the reconstructed field illuminated in the DOI. Repeating the same procedure for all the transmitters of the array, it can be obtained the incident field needed in the imaging algorithm.

III. EXPERIMENTAL RESULTS

A. Calibration Implementation

In this study, the calibration is applied to the MWI brain stroke system in [10], including an array of twenty-four printed monopole antennas conformal to the upper part of the head. Each antenna is embedded in a brick of matching medium (MM), namely a custom-made mixture of urethane rubber and graphite powder [14]. A two-port vector network analyzer (VNA) allows to acquire scattering data in the device's working frequency range 0.9-1.1 GHz [15]. Moreover, the reference experimental scenario is a realistic head phantom uniformly filled with brain tissues-mimicking liquid (having permittivity and conductivity equal to 45.38 and 0.77 S/m at 1 GHz, respectively). The numerical component is realized through a full-wave simulation software based on the finite
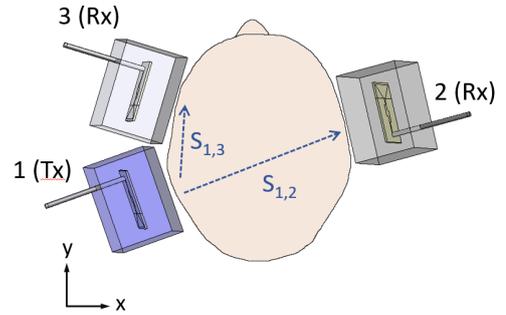

Fig. 1. Model of the experimental setup, with one transmitting (Tx) antenna and two receivers (Rx) of the array used in [10].
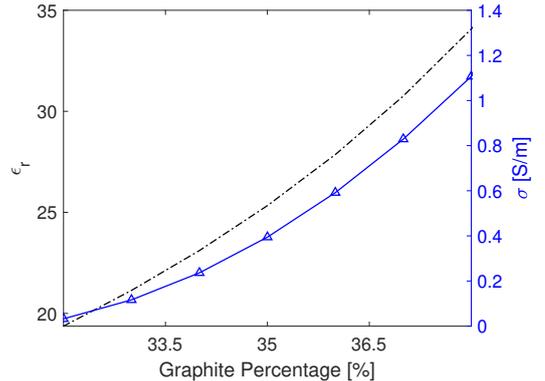

Fig. 2. Experimental characterization of the antennas matching medium (MM) permittivity, ϵ_r, and conductivity, σ, varying the graphite percentage within the mixture with respect to a nominal value of 35%.

element method (FEM) [12], which receives in input the 3-D CAD model mesh, and computes the S-parameters at the antenna ports, together with the radiated electric field within the DOI.

Here, we apply the calibration on measured TCs between one Tx antenna and two different receivers, one close to the transmitter, and the other one opposite to it (as depicted in Fig. 1). Testing these limit conditions, then the outcomes can be reasonably extended to the entire scattering matrix characterizing the array.

To build the simulated basis functions, it is required to properly select the "uncertain" parameters and their range of variation, aiming to describe a space of solutions able to reconstruct the measured data. Thus, starting from the experimental consideration given in [13], three parameters, that influence the antenna behaviour, are analyzed: the air gap separating the antennas from the head, and the MM permittivity and conductivity. However, the first one is found to minimally affect the transmission between different array elements, thus, it is neglected here.

Rather, the dielectric properties deviations are selected on the basis of the experimental characterization summarized in Fig. 2, showing the effects of different percentages of graphite in the MM mixture, forced to emulate possible inaccuracies during the manufacturing process. It can be observed that
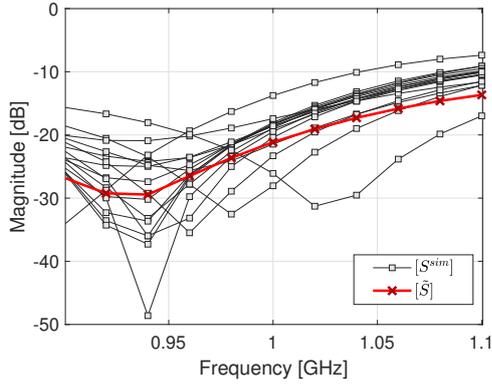
Fig. 3. Simulated set of reflection coefficients for one antenna used for the construction of the basis ($[S^{sim}]$), with the correspondent measured data $[\tilde{S}]$.
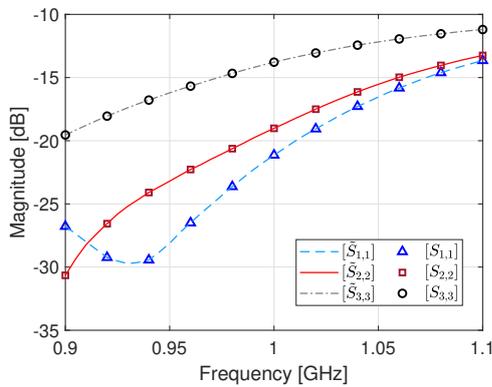

Fig. 4. Reconstruction of the reflection coefficients of three different antennas in [0.9-1.1] GHz: the lines are the measured data $[\tilde{S}_{n,n}]$, while the markers are the reconstructed samples $[S_{n,n}]$.

a graphite increase of 1% from the central nominal value (equal to 35%) produces a 10% increase of the permittivity and a 50% increase of the conductivity. Furthermore, once the antennas reflection coefficients (RCs) are measured, the dielectric values can be specifically tuned to match the actual operating conditions of each antenna. Accordingly, the simulated functions are defined by scaling the nominal permittivity and conductivity by factors within [0.9-1.6] and [0.8-2.5], respectively; for example, Fig. 3 shows the RCs shifts included in the synthetic dataset for a single antenna, compared to the measured reflection coefficient.

Firstly, it should be verified the capability of the derived basis to reconstruct the antennas reflection behaviour. Then, all the selected antennas variations are combined in the transmission basis, proceeding with the TCs reconstruction. Note that the number of basis should be optimized with respect to the variability of the parameters of interest experimentally observed, since it greatly affects the computational time of the procedure. For this purpose, the singular values of the matrix in Eq. 2 are used to select the most significant information.
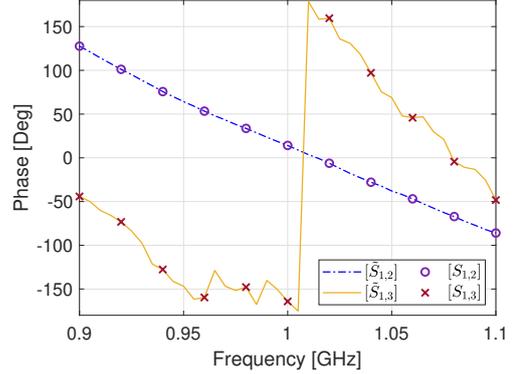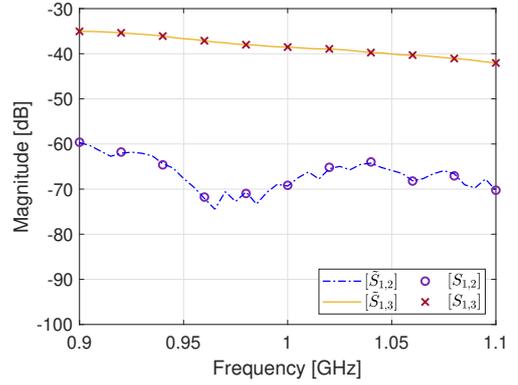

Fig. 5. Reconstruction of the transmission coefficients magnitude (top) and phase (bottom) between the transmitting antenna and two receivers depicted in Fig. 1. The reconstructed samples $[S_{n,m}]$ (markers) almost perfectly overlap the measurements $[\tilde{S}_{n,m}]$ (lines).

B. Measured S-Parameters Reconstruction

In the following, the results of the calibration scheme applied to the reduced array's scattering measurements are presented. The first condition to fulfill is the reconstruction of the RCs of each operating antenna, $[S_{n,n}]$. As shown in Fig. 4, all the samples within [0.9-1.1] GHz are very well reconstructed. Here can be noticed the actual variability of the real antennas characteristics, although the considered array elements are designed to be identical, as it would be in the not calibrated EM modelling. Then, the transmission between the examined antennas pairs, $[S_{1,2}]$ and $[S_{1,3}]$ (see Fig. 1), are depicted in Fig. 5, where both the S-parameters magnitude (top) and phase (bottom) are analyzed. It is evident that both the phase and the amplitude of the transmission parameters are well reconstructed by the generated basis.

IV. CONCLUSION AND PERSPECTIVES

This study further validates the HS-M calibration procedure introduced in [13], proving its potential for the reconstruction of the scattering parameters measured through a real MWI system. Combining a priori information on the antenna array, it is identified a specific set of basis functions that allows to recover the physical behaviour of the device under test, compensating the observed differences with respect to the

nominal numerical model (specifically due to manufacturing inaccuracies).

In the light of the experimental results reported in this paper, it is planned to apply the calibration at the entire antennas array in order to obtain the "measure-matched" incident electric field inside the DOI: this is expected to improve the imaging operator reliability and, consequently, the imaging outcome.

REFERENCES

[1] N. K. Nikolova, *Introduction to Microwave Imaging*. EuMA High Frequency Technologies Series, Cambridge University Press, 2017.

[2] M. Bertero and P. Boccacci, *Introduction to inverse problems in imaging*. CRC press, 2020.

[3] O. Karadima, M. Rahman, I. Sotiriou, N. Ghavami, P. Lu, S. Ahsan, and P. Kosmas, "Experimental validation of microwave tomography with the DBIM-TwIST algorithm for brain stroke detection and classification," *Sensors*, vol. 20, no. 3, 2020.

[4] A. Zakaria, C. Gilmore, and J. LoVetri, "Finite-element contrast source inversion method for microwave imaging," *Inverse Problems*, vol. 26, no. 11, 2010.

[5] R. Scapaticci, J. A. Tobon Vasquez, G. Bellizzi, F. Vipiana, and L. Crocco, "Design and numerical characterization of a low-complexity microwave device for brain stroke monitoring," *IEEE Trans. Antennas Propag.*, vol. 66, pp. 7328–7338, Dec. 2018.

[6] P. Meaney, K. Paulsen, and J. Chang, "Near-field microwave imaging of biologically-based materials using a monopole transceiver system," *IEEE Transactions on Microwave Theory and Techniques*, vol. 46, no. 1, pp. 31–45, 1998.

[7] M. Ostadrahimi, P. Mojabi, C. Gilmore, A. Zakaria, S. Noghanian, S. Pistorius, and J. LoVetri, "Analysis of incident field modeling and incident/scattered field calibration techniques in microwave tomography," *IEEE Antennas and Wireless Propagation Letters*, vol. 10, pp. 900–903, 2011.

[8] S. Tu, J. McCombe, D. Shumakov, and N. Nikolova, "Fast quantitative microwave imaging with resolvent kernel extracted from measurements," *Inverse Problems*, vol. 31, no. 4, 2015.

[9] G. Giordanengo, M. Righero, F. Vipiana, G. Vecchi, and M. Sabbadini, "Fast antenna testing with reduced near field sampling," *IEEE Transactions on Antennas and Propagation*, vol. 62, no. 5, pp. 2501–2513, 2014.

[10] J. A. Tobon Vasquez, R. Scapaticci, G. Turvani, G. Bellizzi, D. O. Rodriguez-Duarte, N. Joachimowicz, B. Duchêne, E. Tedeschi, M. R. Casu, L. Crocco, and F. Vipiana, "A prototype microwave system for 3d brain stroke imaging," *Sensors*, vol. 20, no. 9, 2020.

[11] D. O. Rodriguez-Duarte, J. A. Tobon Vasquez, R. Scapaticci, G. Turvani, M. Cavagnaro, M. R. Casu, L. Crocco, and F. Vipiana, "Experimental validation of a microwave system for brain stroke 3-d imaging," *Diagnostics*, vol. 11, no. 7, 2021.

[12] D. O. Rodriguez-Duarte, J. A. Tobon Vasquez, R. Scapaticci, L. Crocco, and F. Vipiana, "Assessing a microwave imaging system for brain stroke monitoring via high fidelity numerical modelling," *IEEE Journal of Electromagnetics, RF and Microwaves in Medicine and Biology*, vol. 5, pp. 238–245, Sept. 2021.

[13] D. O. Rodriguez-Duarte, J. A. Tobon Vasquez, and F. Vipiana, "Hybrid simulation-measurement calibration technique for microwave imaging systems," in *2021 15th European Conference on Antennas and Propagation (EuCAP)*, pp. 1–5, 2021.

[14] D. O. Rodriguez-Duarte, J. A. T. Vasquez, R. Scapaticci, L. Crocco, and F. Vipiana, "Brick-shaped antenna module for microwave brain imaging systems," *IEEE Antennas and Wireless Propagation Letters*, vol. 19, no. 12, pp. 2057–2061, 2020.

[15] Keysight Technologies, "Keysight streamline series USB vector network analyzer P937XA 2-port, up to 26.5 GHz," *Data Sheet*, Oct. 2018.